

No X-ray Bright Type II Quasars Among the Lyman- α Emitters

S. Malhotra¹, J. X. Wang², J. E. Rhoads¹, T. M. Heckman², C. A. Norman^{1,2}

ABSTRACT

The Lyman- α emitters found at $z=4.5$ and 5.7 by the Large Area Lyman Alpha (LALA) survey have high equivalent widths in the Lyman- α line. Such lines can be produced by narrow-lined active galactic nuclei (AGNs) or by stellar populations with a very high proportion of young, massive stars. To check for Type-II (i.e., narrow-lined) quasars, we obtained a deep X-ray image of 49 Lyman- α sources in a single field of the ACIS instrument on the Chandra X-ray Observatory. None of these sources were detected with a 3σ limiting X-ray luminosity of 2.9×10^{43} ergs/s. For comparison, the two known high redshift type-II quasars have luminosities of 4×10^{43} ergs/s before extinction correction. The sources remain undetected in stacked images of the 49 Lyman- α sources (with 6.5 Ms effective *Chandra* on-axis exposure) at 3σ limits of 4.9×10^{42} . The resulting X-ray to Lyman- α ratio is about 4-24 times lower than the ratio for known type-II quasars, while the average Lyman- α luminosity of the LALA sample is in between the two type-II's. The cumulative X-ray to Lyman- α ratio limit is also below that of 90% of low-redshift Seyfert galaxies.

Subject headings: none supplied

1. Introduction

A large population of high redshift AGNs would have interesting implications both for the pace of black hole formation and growth in the universe and for cosmic background radiations from the gamma ray to the far infrared. Of particular interest is the possibility of a large population of type II quasars, i.e., systems whose broad line regions and soft x-rays are greatly attenuated by large column densities of gas and dust. Population synthesis models

¹Space Telescope Science Institute, 3700 San Martin Drive, Baltimore, MD 21218; san@stsci.edu, rhoads@stsci.edu

²Department of Physics and Astronomy, Johns Hopkins University, Baltimore, MD 21218; jxw@pha.jhu.edu, heckman@pha.jhu.edu, norman@stsci.edu

of active galactic nuclei that are built to explain soft and hard X-ray source counts and backgrounds predict that such objects comprise as much as 90% of the high redshift quasar population (e.g., Gilli, Salvati, & Hasinger 2001). The first X-ray selected type II quasars have recently been found (Norman et al 2002, Stern et al. 2002). These type II quasars show prominent, narrow Lyman- α emission lines, comparable in luminosity ($2\text{-}18 \times 10^{42}$ ergs/s) to the LALA sample ($> 4 \times 10^{42}$ ergs/s).

The equivalent widths of Lyman- α emitters selected using narrow-band surveys tend to be large (Malhotra & Rhoads 2002 - hereafter MR02, Kudritzki et al. 2000). The median equivalent width of the Lyman- α line is greater than 200 Å— in a sample of 160 Lyman- α emitters at $z=4.5$ and 18 at $z=5.7$ (MR02, RM01). Normal stellar populations can produce Lyman- α emission with equivalent width 240 Å or less (Charlot & Fall 1993), unless they have a top-heavy initial mass function (IMF), zero (or very low) metallicity, and/or extreme youth (age $< 10^7$ years). The high equivalent widths could also be explained if active galactic nuclei (AGNs) were present in our Lyman- α emitter sample. However, neither narrow-band imaging nor spectroscopy shows evidence of broad emission lines, which rules out classical quasars. Inspired by the recent discovery of type-II quasars, we use deep x-ray imaging to search for type II quasars among the Lyman- α emitters.

2. Observations

3. Optical Data and Sample Selection

The LALA survey comprises two fields, located in Boötes (at 14:25:57 +35:32 J2000.0) and in Cetus (at 02:05:20 -04:55 J2000.0). Each field is 36×36 arcminutes in size, corresponding to a single field of the 8192x8192 pixel Mosaic CCD cameras at the National Optical Astronomy Observatory's 4 meter telescopes. The X-ray observations described in this *Letter* are in the Boötes field. In this field, we have LALA survey data in a total of eight narrowband filters. Five are partially overlapping narrow band filters covering $4.37 < z < 4.57$ for Lyman- α . There are also two non-overlapping filters of similar width covering $5.67 < z < 5.80$ ($\lambda_c \approx 8150$ and 8230Å). Imaging data reduction followed the methods described by Rhoads et al (2000), and Lyman- α candidates were selected using criteria described by RM01 This resulted in Boötes field samples of ≈ 160 good candidates at $z \approx 4.5$ (see Rhoads et al 2000; MR02) and 18 at $z \approx 5.7$ (Rhoads & Malhotra 2001). The Chandra field was placed to maximize the number of large equivalent width sources within the ACIS-I field of view.

3.1. Chandra imaging

A total of 178 kilo-second exposure, composed of two individual observations, was obtained using the Advanced CCD Imaging Spectrometer (ACIS) on the *Chandra X-ray Observatory* in very faint (VFaint) mode. The first observation, with 120 ks exposure, was taken on 2002-04-16/17 (*Chandra* Obs ID 3130). The second observation, with 58 ks exposure, was taken on 2002-06-09 (Obs ID 3482). All four ACIS-I chips and ACIS-S2, ACIS-S3 chips were used, with the telescope aimpoint centered on the ACIS-I3 chip for each exposure. The aimpoint of Obs ID 3130 is 14:25:37.791 +35:36:00.20 (J2000.0), and the aimpoint of Obs ID 3482 is 14:25:37.564 +35:35:44.32, 16'' away from that of Obs ID 3130. Due to their large off-axis angle during the observations, the ACIS-S chips have poorer spatial resolution and effective area than the ACIS-I chips. In this paper, data from any ACIS-S CCD were then ignored.

Data reduction was done with the package CIAO 2.2.1 (see <http://asc.harvard.edu/ciao>). The level 1 data were reprocessed to clean the ACIS particle background for very faint (VFaint) mode observations, and filtered to include only the standard event grades 0,2,3,4,6. All bad pixels and columns were also removed. We excluded high background time intervals from level 2 files, leaving a net exposure time of 172 ks (120 ks from Obs ID 3130, and 52 ks from Obs ID 3482). Three images were extracted from the combined event file: a soft image (0.5 – 2.0 keV), a hard image (2.0 – 7.0 keV) and a total image (0.5 – 7.0 keV). The hard and total bands were cut at 7 keV since the effective area of *Chandra* decreases above this energy, and the instrumental background rises, giving a very inefficient detection of sky and source photons. The average offset between X-ray and optical images was obtained by comparing the X-ray source positions and their optical counterparts (whenever found). Such offset (0.5'') has been corrected for all our analysis in this paper. We ran WAVDETECT (Dobrzycki et al. 1999, Freeman et al. 2002) on the soft, hard, and total band images. A probability threshold of 1×10^{-7} (corresponding to 0.5 false sources expected per image), and scales of 1,2,4,8,16 pixels were used. The detection is down to a limiting flux of 1.6×10^{-16} ergs cm⁻² s⁻¹ in 0.5 – 2.0 keV band, and 1.7×10^{-15} ergs cm⁻² s⁻¹ in 2.0 – 10.0 keV band. Given the uncertainty on the value of the total background, we find that > 65% of the hard X-ray background is resolved to a flux limit of 1.7×10^{-15} ergs cm⁻² s⁻¹ in 2.0 – 10.0 keV band. The detailed results and detected X-ray sources will be published in a future paper (Wang et al. 2003).

3.2. Non-detection of individual sources

Forty nine of the Ly α sources were imaged by the *Chandra* exposure with different effective exposure times. For every X-ray source and Ly α source, we defined a circular source region centered at the source position and with radius R_s set to the 95% encircled-energy radius of *Chandra* ACIS PSF at the position. Note that at larger off-axis angle, we have larger PSF size. Only one Ly α source overlaps any of the X-ray source regions. The 95% encircled-energy radius of *Chandra* ACIS PSF at the overlapped position is $10.2''$, and the corresponding X-ray source and Ly α source are $7.5''$ apart; which is much larger than the 3σ positional error derived from X-ray image ($3.5''$). The number of X-ray pixels encircled by all the X-ray detected source regions is around 80,000, so the probability that one of the 49 Ly α sources fell in an X-ray source region is $\sim 8 \times 10^4 / 5 \times 10^6 \times 49 \approx 78\%$. Thus, the possible coincidence of one X-ray source with one Lyman- α source is not statistically significant.

We also performed X-ray photometry analysis of the 49 Ly α sources. We again used the 95% encircled-energy radius R_s (now centered on the Lyman- α coordinates) as the region to extract source photons, and extracted the background from an annulus with $1.2R_s < R < 2.4R_s$ after masking out nearby sources. We also accounted for differences of exposure time between source regions and background regions (mainly due to CCD edge effects and bad columns). In soft band (0.5 – 2.0 keV), the counts in the source regions for all 49 sources are less than the 90% significance level upper limits of the expected background, with net counts all less than 2.6. In total band (0.5 – 7.0 keV), except for one source with net count of 7.8, all other sources have net counts < 4 , and confidence level $< 90\%$.

The detection of the only source with 7.8 net counts in total band is right at $2\text{-}\sigma$ level. Assuming a powerlaw spectrum with photon index of 1.4 (from the average spectrum of all sources in the field), this implies an X-ray flux of 6.3×10^{-16} ergs $\text{cm}^{-2} \text{s}^{-1}$ in 0.5 – 10.0 keV. The source is detectable by WAVDETECT with a much lower threshold level (10^{-4}), and the distance between the center of the detected X-ray source and the Ly α source is $1.5''$, while the PSF value there is $9''$. However, with a threshold level of 10^{-4} , we expect 0.15 false X-ray source (per X-ray image from WAVDETECT) within $1.5''$ of the 49 Ly α sources, so the statistical significance of the detection remains low. There is no optical continuum counterpart for the possible X-ray source in our broad band optical images. So if real, it should be the counterpart of a Ly α source with an rest-frame equivalent width of $>500\text{\AA}$.

We conclude that except one possible detection at 2σ level in total band, none of the Ly α sources are detected by the X-ray observations. Only upper limits of X-ray fluxes of the Ly α sources can be given. For the Ly α source nearest ($1.8'$) to the axis of X-ray observation, there are no photons within R_s . The 3σ level upper limits of X-ray counts are 6.61 (Gehrels

1986), and the upper limits for X-ray fluxes (for powerlaw spectra with photon index of 1.4) are 1.7×10^{-16} ergs cm $^{-2}$ s $^{-1}$ for soft band, and 4.7×10^{-16} ergs cm $^{-2}$ s $^{-1}$ for total band (0.5 – 10.0 keV). If we use photon index of 2, instead, the above two fluxes will change to 1.9×10^{-16} and 3.3×10^{-16} respectively. Other sources have higher upper limits due to the lower effective areas and larger PSF sizes.

3.3. Cumulative X-rays from all the LALA sources

The X-ray imaging data at the positions of all the Lyman- α sources were stacked, yielding an effective exposure time of 6.5 Ms (75 days). No source was detected in the stacked image in any band (Figure 1). Since Ly α sources have different off-axis angles to the axis of *Chandra* observation, they have different PSF sizes at each position, making it hard to define a source region to do photometry. We just sum up the source counts extracted from each source region, and the expected background counts derived from each background region. In the soft band, we have 55 counts in total in the source regions, and the expected background is 54.2. In the total band, these two numbers are 164 and 163.1 respectively. It is clear that we did not detect the sources in X-ray even after stacking them. The 3σ upper limits of soft and total band net counts are 26 and 42. Assuming a powerlaw spectrum with photon index of 1.4, we have 3σ upper limits of 1.8×10^{-17} ergs cm $^{-2}$ s $^{-1}$ in the 0.5 – 2.0 keV band, and 7.9×10^{-17} ergs cm $^{-2}$ s $^{-1}$ in the 0.5 – 10.0 keV band. For a photon index of 2, these limits translate to 1.9×10^{-17} ergs cm $^{-2}$ s $^{-1}$ and 5.5×10^{-17} ergs cm $^{-2}$ s $^{-1}$.

4. Discussion and conclusions

From the measurements of the X-ray background and from number counts of X-ray sources, one can argue that only a small fraction of Lyman- α emitters can be X-ray bright type-II quasars. Suppose a fraction f of our sources were type-II quasars, i.e., much like CDF-S202 source and distributed in redshift span Δz . The known type-IIs are at $z=3.3$ and 3.7. If these sources and the LALA objects at $z = 4.5$ and 5.7 represent the same population, it would imply $\Delta z > 2.4$. The number counts of objects brighter than CDF-S202 and CXO52 in the hard band in one ACIS field is about 160, while there are 49 Lyman- α sources at $z = 4.47 \pm 0.1$ in the same solid angle. This implies immediately that not more than 27% of the LALA sources should be detectable in our X-ray survey. Even if we deem type II quasars irrelevant to this estimate, given the non-detection of LALA sources; Lyman- α sources have been found at $z=3.1$ with number densities comparable to the LALA determinations (Kudritzki et al. 2000) making $\Delta z = 2.6$.

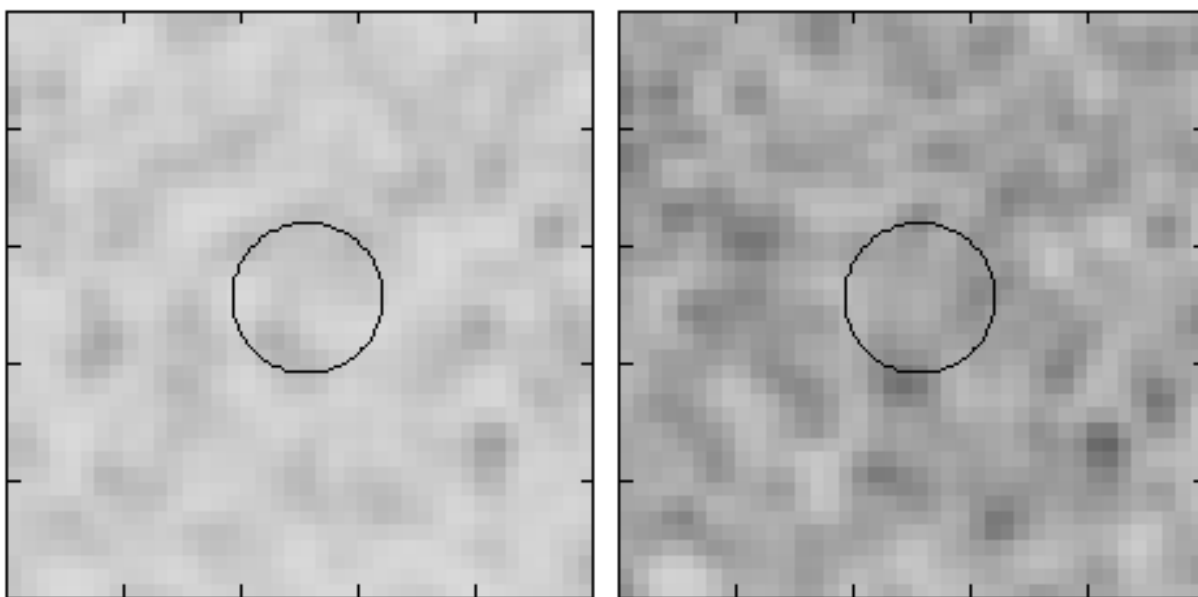


Fig. 1.— Stacked *Chandra* images of 49 $\text{Ly}\alpha$ sources. Left: soft band (0.5 – 2.0 keV); Right: total band (0.5 – 7.0 keV). The effective exposure time of the stacked images is 6.5 Ms. The images are 40×40 pixels in size, and the circles are centered on the stacking position and have a radius of 5 pixels. 1 pixel = $0.492''$. The images were smoothed using program provided by CIAO.

Assuming we have a type II AGN at $z=4.5$, with intrinsic photon index of 2, but heavily absorbed, $N_H = 10^{24} \text{ cm}^{-2}$, $H_0 = 65 \text{ km s}^{-1} \text{ Mpc}^{-1}$, $\Omega_m = 1/3$, $\Omega_\lambda = 2/3$. The best $3\text{-}\sigma$ upper limits of 0.5 – 7.0 keV band net count at individual LALA locations correspond to a type II AGN with 2.0 – 10.0 keV rest frame intrinsic luminosity of $1.5 \times 10^{44} \text{ ergs s}^{-1}$. And for stacked images, this number is $2.5 \times 10^{43} \text{ ergs s}^{-1}$. The rest frame intrinsic luminosity of CDFS-202 is $8.0 \times 10^{44} \text{ ergs s}^{-1}$ (Norman et al. 2002), and $4.2 \times 10^{44} \text{ ergs s}^{-1}$ for CXO52 (Stern et al. 2001). See Table 1 for corresponding luminosities with no extinction correction applied.

However, if we were to scale the X-ray fluxes with Lyman- α line flux, which in most cases is the only well measured property of the LALA sources, we find that about 44 out of 49 sources would have been detected had they been like CDF-S202. About 3 sources like CXO52 would have been detected by these observations. Figure 2a shows the comparison, where the ratio of X-ray 3σ upper limits to Lyman- α line flux for LALA sources is shown as a histogram and the values of this ratio for the two known type-II quasars are marked. The spread in the histogram is due to variation in x-ray flux sensitivity and the variation in Lyman- α line strength. Also shown is this ratio for cumulative LALA source positions which is 4-24 times lower than either of the known QSO-IIs. The $3\text{-}\sigma$ upper limit of average X-ray flux from each source is $5.5 \times 10^{-17} \text{ ergs cm}^{-2} \text{ s}^{-1}$ in the 0.5–10 KeV band, compared to a few $\times 10^{-15} \text{ ergs cm}^{-2} \text{ s}^{-1}$ for the two known type-II quasars. Comparison with relatively lower luminosity, low redshift ($z < 1$) Seyferts and quasars drawn from the samples of Kriss (1984, 1985) shows that while individually the LALA upper limits are higher than the X-ray/Lyman- α ratio for about half the low- z sample, the upper limits from the stacked LALA positions is lower than 90% of low- z sources (Figure 2b).

Assuming a power-law spectrum with photon index $\Gamma = 2.0$, the 3σ upper limit of 0.5 – 2.0 keV flux on the average LALA sources corresponds to an X-ray luminosity of $4.2 \times 10^{42} \text{ ergs s}^{-1}$ at $z=4.5$ (for either 0.5 – 2.0 keV rest frame or 2.0 – 8.0 keV rest frame bandpass, $H_0=65 \text{ km s}^{-1} \text{ Mpc}^{-1}$, $\Omega_m=1/3$, $\Omega_\lambda=2/3$). The Lyman break galaxies at $z \simeq 3$ have an average luminosity of $6 \times 10^{40} \text{ ergs s}^{-1}$ (after excluding the four known AGNs) which is consistent with their being starbursts with star-formation rates of about $60 M_\odot \text{ yr}^{-1}$ (Nandra et al 2002, Brandt et al. 2001). Clearly, our observations are not sensitive enough to detect starbursts (nor were they designed to be). Taking the difference in star-formation rates between Lyman- α selected galaxies and LBGs into account and adopting the LBG value for the ratio of star formation to X-ray emission, we should expect an average x-ray luminosity of $\approx 6 \times 10^{39} \text{ ergs s}^{-1}$.

Could some of the Lyman- α sources still be AGNs? We have demonstrated that X-ray bright quasars are at most a minority of the LALA objects. Our composite nondetection

implies that even at the 3σ level, only a few percent of LALA sources could resemble CDF-S202, and $< 25\%$ could resemble CXO52. The most plausible way to have luminous AGN hiding in the LALA sample without violating this constraint is to suppose that they are Compton-thick, so that even relatively hard X-rays are obscured. Thermal emission from the obscuring dust would render these objects detectable in the infrared or submillimeter.

Another test relies on optical spectra. The Lyman- α line is found to be narrow ($< 500\text{kms}^{-1}$) in all our spectroscopically confirmed Lyman- α emitters (e.g., Rhoads et al. 2000, Rhoads et al. 2002), which is narrower than the typical physical line widths of even type II quasars. For the larger fraction of Lyman- α sources which are photometrically selected using narrow-bands 80 Å wide, we can also rule out velocities $> 3700\text{kms}^{-1}$. Steidel et al (2002) find at least one case of narrow-lined AGN in their Lyman-break galaxy sample with x-ray luminosity $< 5 \times 10^{42}$ ergs s^{-1} . Their identification of this source as an AGN is based on the detection of narrow lines of NV, CIV, HeII and CIII in emission. None of the spectra of Lyman- α emitters shows these lines. In conclusion, we find no evidence for AGN among the Lyman- α emitters found in the LALA survey.

This work has benefitted from images provided by the NOAO Deep Wide-Field Survey (NDWFS; Jannuzi and Dey 1999), which is supported by the National Optical Astronomy Observatory (NOAO). NOAO is operated by AURA, Inc., under a cooperative agreement with the National Science Foundation. We also thank the referee for a prompt and helpful report.

REFERENCES

- Brandt, W. N., Hornschemeier, A. E., Schneider, D. P., Alexander, D. M., Bauer, F. E., Garmire, G. P., Vignali, C. 2001, ApJ 558, L5
- Charlot, S. & Fall, S. M. 1993, ApJ, 415, 580
- Dobrzycki et al. 1999, Chandra Detect 1.0 user guide. Chandra X-ray center, Cambridge.
- Freeman, P.E., Kashyap, V., Rosner, R., & Lamb, D. Q., 2002, ApJS, 138, 185
- Gehrels, N. 1986, ApJ 303, 336
- Gilli, R., Salvati, & Hasinger, G. 2001, A&A, 366, 407
- Jannuzi, B. T., & Dey, A., 1999, in “Photometric Redshifts and High Redshift Galaxies,” ASP Conference Series, Vol. 191, editors R. J. Weymann, L. J. Storrie-Lombardi, M. Sawicki, and R. J. Brunner, p.111

- Kriss, G. A. 1984, ApJ 277, 495
- Kriss, G. A. 1985, AJ 90, 1
- Kudritzki, R.-P. et al. 2000, ApJ, 536, 19
- Malhotra, S. & Rhoads, J.E. 2002, ApJ, 565, L71
- Nandra, K., Mushotzky, R. F., Arnaud, K., Steidel, C. C., Adelberger, K. L., Gardner, J. P., Teplitz, H. I., Windhorst, R. A. 2002, ApJ 576, 625
- Norman, C. et al. 2002, ApJ, 571, 218
- Rhoads, J. E., Malhotra, S., Dey, A., Stern, D., Spinrad, H., & Jannuzi, B. T. 2000, ApJ, 545, L85
- Rhoads, J. E. & Malhotra, S. 2001, ApJ563, L5
- Rhoads, J. E. et al. 2002, accepted to AJ
- Stern, D et al. 2002, ApJ568, L71
- Steidel, C. et al 2002, ApJ, 576, 653
- Wang, J.X. et al. 2003, in preparation.

Table 1. X-ray flux and Luminosity measurements and limits

Object Type	Flux ergs cm ⁻² s ⁻¹	Luminosity (2-10 keV) ergs s ⁻¹
Individual Lyman- α emitters	$< 3.3 \times 10^{-16}$	$< 2.9 \times 10^{43}$
Coadded Lyman- α emitters	$< 5.5 \times 10^{-17}$	$< 4.9 \times 10^{42}$
Type II quasar: CDF-S202	$2.3 - 2.8 \times 10^{-15}$	4.4×10^{43}
Type II quasar: CXO-52	1.8×10^{-15}	3.6×10^{43}
Lyman Break Galaxies (Coadded non-AGN)	4×10^{-18}	6×10^{40}
Lyman- α galaxies if starbursts		6×10^{39}

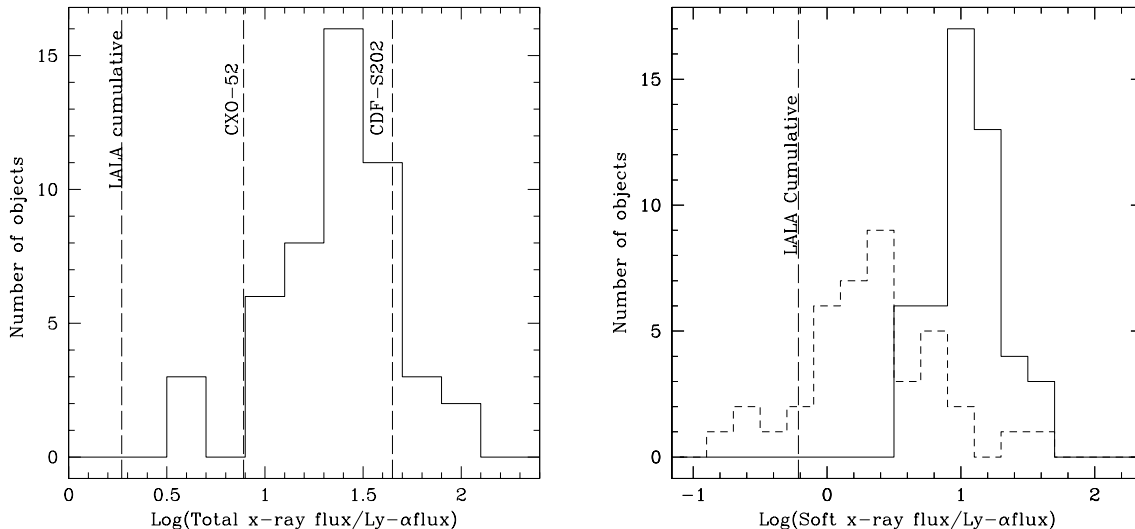


Fig. 2.— Comparison of X-ray to Lyman- α flux ratios: Figure 2a shows the comparison of this ratio for the 49 Lyman- α emitters at $z=4.5$ from the LALA sample with high redshift Type-II quasars. We use $3\text{-}\sigma$ upper limits derived for the total band since there are no detections. The vertical bars mark the observed ratio for the two known high redshift type-II quasars (see text), and the $3\text{-}\sigma$ upper limit for all the Lyman- α sources stacked. Since the photon indices of the known type-II quasars are different from the assumed photon index for the undetected Lyman- α emitters, we have adjusted the x-ray fluxes in all sources as if the photon index were $\Gamma = 2$. Figure 2b shows comparison with low-redshift ($z < 1$) Seyfert galaxies and quasars (Kriss 1984, 1985). The solid histogram is as in Figure 2a, except we plot the soft band (0.5–2.0 keV, observed; 2.75–11 keV, rest) and the dashed histogram is the comparison sample from Kriss (1984 & 1985) adjusted to rest-frame 2.75–11 keV. The $3\text{-}\sigma$ upper limit on the stacked Lyman- α sources is shown as a vertical bar.